In: Proceedings of the 38th Asilomar Conference on Signals, Systems, and Computers, Pacific Grove CA, Nov. 7-10, 2004.

SYNTHETIC APERTURE RADAR VISUALIZATION

Randolph L. Moses, Emre Ertin, and Christian Austin

Department of Electrical and Computer Engineering
The Ohio State University
2015 Neil Avenue
Columbus, OH 43210 USA

ABSTRACT

We investigate methods for two-dimensional and three-dimensional reconstruction of objects from radar backscatter measurements taken over wide angles. Radar backscattering is characterized by several variables: object location, complex amplitude, polarization, and the aspect (azimuth and elevation) of the interrogating sensor. This high-dimensional data is typically projected into a two-dimensional image. As next-generation radar systems become increasingly capable, the assumptions and algorithms for traditional imaging need to be reconsidered. We propose new imaging techniques that accommodate limited persistence scattering on objects, and use these techniques to develop two-dimensional and three-dimensional object reconstructions from wide-aperture radar measurements. Finally, we explore phase and polarization stability of scattering centers at the high resolutions afforded by wide-angle apertures.

1. INTRODUCTION

This paper considers techniques for processing and displaying radar backscatter measurements of an object taken over one or more wide-angle apertures. An aperture is considered to be "wide-angle" if its angular extent exceeds that needed to produce synthetic aperture radar (SAR) imagery whose image resolution is equal in both downrange and crossrange. We consider both two-dimensional image reconstructions and three-dimensional reconstructions based on interferometric SAR (IFSAR) apertures.

Recent technology advances motivate consideration of wide angle imaging. Advances in inertial navigation systems and in global positioning systems permit collection of radar backscatter data that is coherent over larger apertures. In addition, bistatic radar systems are becoming increasingly popular; in bistatic systems a standoff transmitter illuminates a scene of interest, and an aircraft receives backscatter from the scene. In many cases, the receiver may be an unmanned air vehicle that can fly close to the scene of interest and traverse wide angles around the scene in relatively short time periods. Finally, multiple pairs of radar transmitters and receivers can interrogate a scene; if the data collections are coherent, several smaller apertures can be combined to form wide-angle apertures.

Wide-angle data collections are also possible in some inverse SAR (ISAR) applications, in which object motion is used to obtain aspect diversity of backscatter measurements. If object motion induces large angular changes (such as when the object is rotating), wide-angle aperture data collections are possible.

Our preliminary investigations of object reconstructions from wide-angle apertures have motivated consideration of two hypotheses. First, object scattering behavior over wide angles is not well-modeled by small-angle scattering assumptions that form the basis of most current object reconstruction methods. We hypothesize that most scattered energy from objects of interest have limited angles of persistence, and that such limited-persistence scattering motivates revisiting traditional assumptions and algorithms for reconstructing objects in 2D or 3D. In particular, standard backprojection-based SAR imaging implicitly assumes that scattering responses persist over the entire data collection aperture, and that assumption does not appear to hold for most of the backscattered energy from typical ground vehicles at X-band frequencies. Second, at sufficiently high resolutions, scattering centers on the object become resolved, and resolved scattering center responses have both stable phase responses and stable polarimetric response properties. As a result, 3D location information inferred from scattering phase is sufficiently stable to permit 3D object reconstructions using IFSAR, and polarimetric features extracted from scattering centers are useful features to describe local geometry of the object. In addition, techniques for resolution enhancement become (much) more stable.

In this paper we present qualitative evidence to support the above two hypotheses. In addition, we explore an alternative approach to 2D object imaging from wide-angle apertures which is better matched to a limited-persistence scattering assumption. We present initial results on 2D resolution enhancement from wide-angle, narrowband data. Fi-

nally, we explore 3D object reconstruction from sparse wide angle apertures, and explore both angle and polarization features for enhancing object reconstruction and recognition.

2. GLRT IMAGE FORMATION

Traditional techniques for radar images formation relies on a point-scattering assumption; that is, scattering centers have responses whose amplitude is not a function of frequency or angle, and whose phase encodes the (x, y, z) location of the scattering center. In fact, backprojection image formation can be interpreted as a matched filter for point scattering responses [1]. At small fractional bandwidths and narrow apertures that are traditionally used for radar imaging, the point scattering assumption often serves as a good approximation; however, for wide-angle apertures, this may not be the case. In fact, studies have shown that few scattering centers persist for angles exceeding 20° at X-band [2]. The matched filter corresponding to wide-aperture imaging is not well-matched to limited-persistence scattering, and the response of a scattering center that persists over a narrow angle may appear as a low-amplitude response in the image, because the image averages the response over the entire wide-angle azimuth aperture.

An alternate approach is to use a bank of matched filters, each characterized by a center response azimuth and a response width and shape. Such matched filters have been proposed for detection in wide-angle, low-resolution imagery [3, 4], and we propose to consider a similar approach for object image formation. That is, we propose to model the aspect response of a scattering center as

$$r(\phi; \phi_c, \Delta) = r_0\left(\tfrac{\phi-\phi_c}{\Delta}\right) \tag{1}$$

for a given generic response shape r_0. We propose forming a SAR image whose response at location (x, y) on the image is the Generalized Likelihood Ratio Test (GLRT) matched filter output for scattering centers with unknown center azimuth and width; that is:

$$I(x, y) = \max_{\phi_c, \Delta} I(x, y; \phi_c, \Delta) \tag{2}$$

where $I(x, y; \phi_c, \Delta)$ is the SAR image formed using an aperture centered at angle ϕ_c and with aperture width Δ. In practice, SAR imaging incorporates a window function to reduce response sidelobes in the image at the expense of a slight loss of resolution; the scattering response shape $r_0(\phi)$ can be incorporated into the window design for the formed images.

In this paper, we consider a computationally simpler alternative in which we fix the persistence angle Δ and maximize only over the center aperture ϕ_c; that is,

$$I(x, y) = \max_{\phi_c} I(x, y; \phi_c, \Delta_0) \tag{3}$$

In the cases presented below, we fix $\Delta_0 = 20^\circ$, based on earlier studies of scattering center persistence and on our independent tests using X-band backscatter predictions of ground vehicles.

2.1. GLRT Imaging Examples

To support wide-angle object reconstruction experiments, we use scattering prediction data of a backhoe. The data is generated using the XpatchF scattering prediction software. A full 'data dome' of monostatic, full polarization backscatter predictions have been generated at frequencies from 7–13 GHZ, measured from an incidence angle from 0–360° in azimuth and 0–90° in elevation, taken in $1/14^\circ$ steps.

To illustrate the GLRT imaging approach, we consider wide angle images formed from a two-dimensional slice of the backhoe data dome. The data consists of a linear aperture with a 110° azimuth aperture centered at 45°, and with a peak elevation angle of $\theta = 30^\circ$. The elevation angle tapers at each end of the aperture to emulate a straight-line radar flight path (constant aircraft elevation above ground) such that the elevation angle at the closest point to the object is 30°. The data has a center frequency of $f_c = 10$ GHz; bandwidths of 4 GHz and 500 MHz about this center frequency were used to form images.

Figure 1 shows both 4GHz and 500MHz images of the backhoe using standard polar format algorithm (PFA) image formation techniques, and using a Hamming window in both the frequency and azimuth directions. Color encodes response radar cross section (RCS) amplitude in dB, with the top 40 dB responses shown. The radar center aperture is at the top of these images. Figure 2 shows the backhoe at an angle that corresponds approximately to the image-plane projection for the images in Figure 1 (and also for Figures 3–5 below).

Figure 3 shows the results of the GLRT imaging approach in equation (3). Each pixel in the image shows the GLRT image output from equation (3), where for simplicity we have fixed the scattering persistence width of $\Delta_0 = 20^\circ$ and we have quantized ϕ_c at 5° increments from 0–90°. We note that the images formed in Figure 3 have a simple computational form. We form 19 standard 20°-azimuth subimages centered at $\phi_c = 0^\circ, 5^\circ, \ldots, 90^\circ$ and display, at each pixel, the maximum amplitude from these 19 subimages.

For GLRT imaging, each position (x, y) of the image is characterized by additional information that is not available in full-aperture imaging: namely, the center angle ϕ_c found in the maximization process in equation (3) (if equation (2) is used, Δ is an additional feature). These parameters may be useful as features for visualization or recognition of objects. To illustrate this point, Figure 4 shows the GRLT images from Figure 3, but in this case color for each image pixel is used to encode the angle ϕ_c at which the maximum in equation (3) occurs. The coloring of angle is shown in the "rainbow" in the images (red corresponds to $\phi_c = 0^\circ$, blue

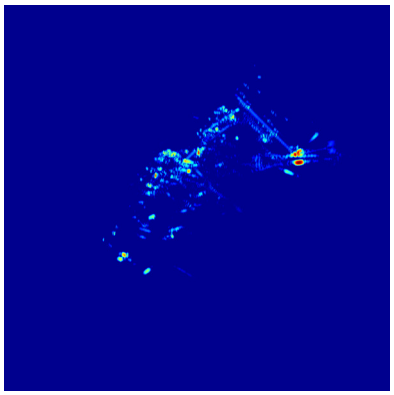

(a) 4 GHz bandwidth

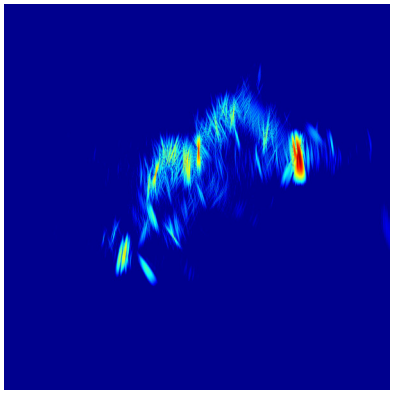

(b) 500 MHz bandwidth

Fig. 1. SAR image of the backhoe using a full 110° linear aperture centered at 45° azimuth; color shows RCS.

corresponds to $\phi_c = 90°$). This angle provides a grouping of pixels, and substructures in the object become distinguishable by color.

It is important to note that the GLRT images shown in Figures 3 and 4 involve *noncoherent combinations* of subaperture imagery. From an operational perspective, noncoherent combinations impose a much lower constraint on data collections. In particular, the individual subimages could be collected by different radar platforms, with no requirement of phase coherence across these platforms.

2.2. Resolution Enhancement

The images in Figures 3(b) and 4(b) show significantly different downrange and crossrange resolutions, indicated by the line-segment-like responses of many of the scattering terms. The length of the line-segments is consistent with the 12-inch downrange resolution determined by the 500 MHz radar bandwidth, and the 2-inch crossrange resolution is consistent with a 20° aperture at a center frequency of 10 GHz (see also [5]). In this section we explore the utility of nonparametric resolution enhancement techniques to improve

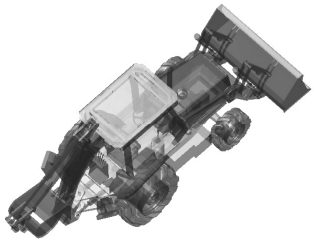

Fig. 2. Backhoe model used in Xpatch scattering predictions.

the downrange resolution for such images.

We note that downrange resolution enhancement is implicitly an attempt at extrapolation of the given radar backscatter data. Downrange resolution enhancement corresponds to bandwidth extrapolation; angle extrapolation is not needed as the 20° subimage azimuth apertures correspond to a crossrange resolution of approximately 2 inches (for scattering centers that persist over the entire 20° aperture). We remark that scattering response is more easily predictable as a function of frequency than as a function of aspect; aspect dependencies such as scattering center shadowing or obscuration by other structures on the object give rise to higher prediction errors in azimuth. In addition, compared to 12×12 inch radar imagery, the number of scattering centers likely to overlap in a resolution cell should be smaller. This suggests that resolution enhancement techniques applied to the subaperture imagery used here may have a greater chance of success than in some applications considered previously.

Figure 5 shows the results of applying a regularized l_p-norm based method proposed by Çetin and Karl [6]. The algorithm is nonparametric and thus somewhat robust to scattering physics assumptions. The technique solves the optimization problem of the form

$$\min_u \left\{ \|Au - b\|^2 + \lambda \|u\|_p^p \right\} \tag{4}$$

where b contains (noisy) samples of the measured scattering, A is the imaging operator, and u is the discretized grid of image amplitudes and phases. Equation (4) may be viewed as a regularization of $Au = b$, in which fidelity to the measured (noisy) phase history is traded against the l_p "energy" penalty of the reconstruction u. Figure 5 shows significant improvement in downrange resolution, when compared to Figure 4(b).

3. IFSAR RECONSTRUCTION

In this section we explore the second hypothesis, namely, that at sufficiently high resolutions, scattering centers on the object become resolved, and resolved scattering center responses have stable phase responses and polarimetric properties.

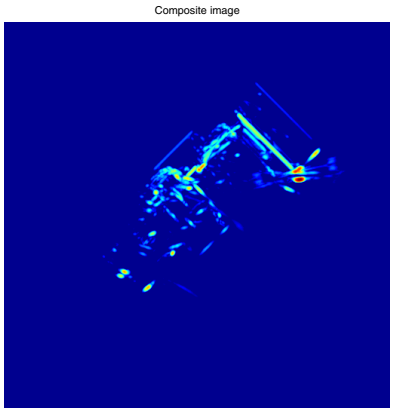

(a) 4 GHz bandwidth

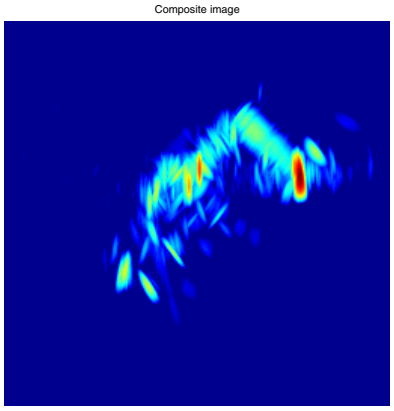

(b) 500 MHz bandwidth

Fig. 3. GLRT SAR image of the backhoe for scattering responses with persistence 20°; color shows amplitude (RCS).

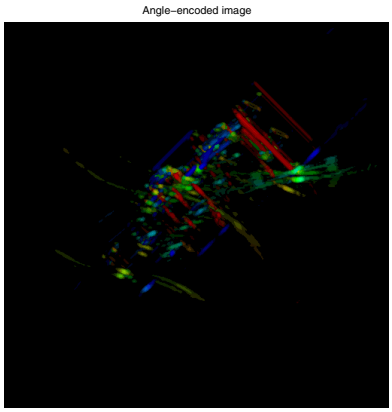

(a) 4 GHz bandwidth

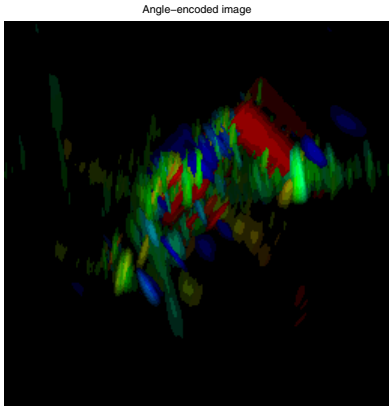

(b) 500 MHz bandwidth

Fig. 4. GLRT SAR image of the backhoe for scattering responses with persistence 20°; color shows the azimuth angle at which each pixel exhibits maximum response.

In particular, we show by example that the phase responses from GLRT subimages are sufficiently stable to permit 3D reconstruction from two closely-spaced (in elevation) apertures via IFSAR processing. In IFSAR imaging, the height of a given scattering center, measured from its image plane, is proportional to the phase difference from two closely-spaced (in elevation) images [7]. If this phase is sufficiently stable, 3D reconstructions can be obtained. We show using backhoe data that for sufficiently high resolutions, scattering centers become isolated in image resolution cells, so that their phase is a stable indicator of scattering center height.

The use of IFSAR for 3D reconstruction provides a significant savings in data collection. Traditional 3D SAR imaging involves measurements of a data "cube", over a range of frequencies, azimuths, and elevations. If 3D reconstruction is possible through IFSAR techniques, then one needs only two closely-spaced elevation slices of this 3D cube; this imposes a much lower cost of data collection than for traditional 3D imaging.

Figure 6 shows a result in which both scattering center phase and polarization features are used in a 3D object reconstruction. Phase is used to compute a 3D location, and color encodes polarization state. In this figure, IFSAR subimage pairs are obtained every 5° in azimuth from 60–120° and for elevations of $5k^\circ$ and $(5k + 0.05)^\circ$, where $k \in 0, \ldots, 12$. Each radar has bandwidth of 4 GHz. Pixels in the top 40 dB of each GLRT subimage pair are used to compute the 3D scattering center location [7]. The polarization matrix of each scattering center is estimated. Figure 6 uses color to encode an angle α that describes a mixture of dihedral (even-bounce) and trihedral (odd-bounce) scattering [8]; here, red denotes purely odd bounce, blue denotes even bounce, and green denotes mixtures. We see good agreement to 3D geometry, and that polarization is useful to segment substructures on the object. We note that polarization features other than α are also available, such as the orientation angle of dihedrals, and these features provide additional information about object substructure shape.

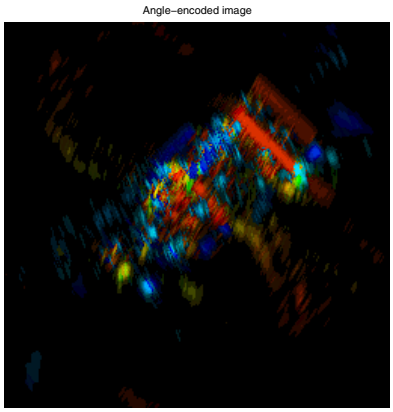

Fig. 5. 500 MHz bandwdith GLRT image using resolution enhancement with $p = 1$ and $\lambda = 0.1$.

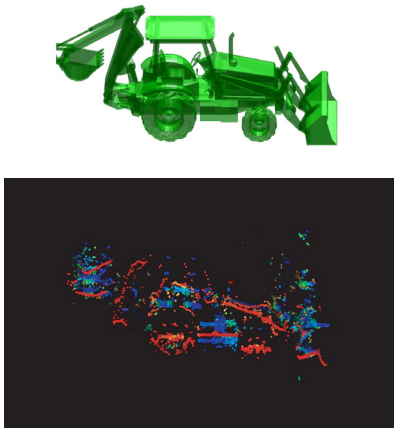

Fig. 6. 3D backhoe reconstruction in which color encodes a polarization feature that describes even-bounce or odd-bounce scattering; red denotes purely odd bounce, blue denotes purely even bounce, and green denotes a mixture.

4. CONCLUSIONS

At sufficiently high resolution, scattering centers of vehicles become isolated, using X-band radar. Once isolated, scattering center phase is sufficiently stable to extract both 3D location information through IFSAR and local object shape information through polarization analysis. Furthermore, wide-angle apertures can provide significant information about object shape and substructure association.

Traditional SAR image formation is not well suited to wide-angle apertures, due to the limited persistence of many scattering centers on the object. We have presented an alternative imaging procedure for wide-angle apertures that is based on a GLRT interpretation of imaging, and is matched to the limited-persistence property of scattering centers. One advantage of the GLRT-based imaging approach is that additional features (*e.g.*, scattering center aspect and persistence angle) are produced in the imaging process, and these features are useful for substructure discrimination and image visualization. We used this wide-angle imaging technique to demonstrate, by example, that scattering centers become sufficiently isolated to enable resolution enhancement using nonparametric reconstruction techniques, and to permit 3D reconstruction from sparse apertures. Finally, we demonstrated that at sufficiently high resolution, polarization signatures of scattering centers become stable indicators of substructure shape.

We have not explored in detail the resolution needed for scattering centers to be sufficiently isolated. For the example considered, 1.5 in resolution appears to be sufficient. In fact, 12×1.5 in downrange$\times$crossrange resolution appears to provide enough isolation to permit effective (downrange) resolution enhancement. Quantitative investigations of this topic is of current interest.

5. REFERENCES

[1] D. Rossi and A. Willsky, "Reconstruction from projections based on detection and estimation of objects," *IEEE Trans. Acoustics, Speech, and Signal Processing*, vol. 32, pp. 886–906, Aug 1984.

[2] D. E. Dudgeon, R. T. Lacoss, C. H. Lazott, and J. G. Verly, "Use of persistant scatterers for model-based recognition," in *Proc. SPIE 2230* (D. A. Giglio, ed.), pp. 356–368, Apr 1994.

[3] M. R. Allen and L. E. Hoff, "Wide-angle wideband SAR matched filter image formation for enhanced detection performace," in *proc. SPIE 2230* (D. A. Giglio, ed.), pp. 356–368, Apr 1994.

[4] R. D. Chaney, A. S. Willsky, and L. M. Novak, "Coherent aspect-dependent SAR image formation," in *proc. SPIE 2230* (D. A. Giglio, ed.), pp. 356–368, Apr 1994.

[5] R. L. Moses, L. Potter, and M. Çetin, "Wide angle SAR imaging," in *Proc. SPIE 5427* (E. G. Zelnio and F. D. Garber, eds.), Apr 2004.

[6] M. Çetin and W. C. Karl, "Feature enhanced synthetic aperture radar image formation based on nonquadratic regularization," *IEEE Trans Image Processing*, vol. 10, pp. 623–631, Apr 2001.

[7] C.V. Jakowatz, D.E. Wahl and P.H. Eichel, *Spotlight-Mode Synthetic Aperture Radar: A Signal Processing Approach*. Boston: Kluwer, 1996.

[8] E. Ertin and L. C. Potter, "Polarimetric imaging for wide band synthetic aperture radar," *IEE Proc. Radar, Sonar, and Navigation*, vol. 145, no. 5, 1998.